ELSEVIER

Journal of Photochemistry and Photobiology A: Chemistry 109 (1997) 195–200

Journal of PHOTOCHEMISTRY AND PHOTOBIOLOGY A: CHEMISTRY

Applicability of the transient grating technique to the investigation of photoinduced processes following second order kinetics

Eric Vauthey *

Institute of Physical Chemistry of the University of Fribourg, Pérolles, CH-1700 Fribourg, Switzerland

Received 5 March 1997

Abstract

The reliability of the transient grating technique to determine the energetics of processes following second order kinetics, such as free ion recombination, is investigated theoretically. As the second order process takes place, the grating of the reactant population becomes anharmonic, complicating the determination of the population dynamics from the time profile of the diffracted intensity. However, the thermal phase grating is anharmonic from the beginning of the reaction, but is harmonic when the process is completed. As a consequence, the energetics of the reaction can be deduced accurately from the maximum amplitude of the diffracted intensity without having to take the anharmonicity of the grating into account, as long as thermal diffusion is slow. To achieve this, the crossing angle of the pump pulses on the sample has to be smaller than 1°. Otherwise, an arduous fitting procedure is required to extract the energetic parameters from the experimental data. © 1997 Elsevier Science S.A.

Keywords: Transient grating technique; Photothermal method

1. Introduction

Over the past decade, the transient grating technique (TG) has been intensively applied to the study of many physical and chemical processes [1] such as electronic energy transport [2,3], diffusion in liquids [4], optical Kerr effect [5,6], excited state dynamics [7,8], rotational diffusion dynamics [9,10] and photoinduced electron transfer [11,12]. In a transient grating experiment, the sample is excited by two spatially crossed and time coincident laser pulses producing an interference pattern. This spatially modulated excitation creates in the sample spatial distributions of ground state, excited states and/or photochemical intermediates and product populations. Consequently, similar modulations of the absorbance A and of the refractive index n are generated. As long as the intensity of the excitation pulses is well below the saturation intensity, these modulations are harmonic [13]:

$$A(x,\lambda_{pr}) = A_0(\lambda_{pr}) + A_1(\lambda_{pr})\cos\left(\frac{2\pi}{\Lambda}x\right) \quad (1a)$$

$$n(x,\lambda_{pr}) = n_0(\lambda_{pr}) + n_1(\lambda_{pr})\cos\left(\frac{2\pi}{\Lambda}x\right) \quad (1b)$$

where x is the direction of the modulation and Λ is the fringe spacing, which depends on the angle of incidence of the excitation pulses and on their wavelength.

The amplitudes of these grating-like distributions, A_1 and n_1, are measured by a third time delayed laser pulse with a wavelength λ_{pr} striking the grating at Bragg angle. According to Kogelnik coupled wave theory [14], the intensity of the diffracted pulse is given by:

$$\eta(\lambda_{pr}) = \frac{I_{dif}(\lambda_{pr})}{I_{inc}(\lambda_{pr})} \cong \left[\left(\frac{1.15A_1(\lambda_{pr})}{2\cos\theta_B}\right)^2 + \left(\frac{\pi n_1(\lambda_{pr})d}{\lambda_{pr}\cos\theta_B}\right)^2\right] \times \exp\left(-\frac{2.3A_0(\lambda_{pr})}{\cos\theta_B}\right) \quad (2)$$

where η is the diffraction efficiency, I_{inc} and I_{dif} are the intensities of the incident and diffracted pulses respectivelty, θ_B is the Bragg angle and d is the sample thickness.

The diffracted intensity is proportional to the concentration of the species responsible for the changes of absorbance and refractive index at the probe wavelength. Therefore, the time dependence of I_{dif} reflects the dynamics of this species as long as the population grating stays harmonic. This is the case for processes following first or pseudo-first order kinetics. In this

* E-mail: Eric.Vauthey@unifr.ch

PII S1010-6030(97)00151-2

case, the decay of the diffracted intensity is twice as fast as the decay of the population. However, if the population decays with higher order kinetics, the reaction is faster at the grating maxima than at the minima and therefore the spatial shape of the grating changes as the reaction proceeds [15]. As a consequence, the grating becomes anharmonic and the time dependence of the diffracted intensity no longer reflects the dynamics of the average concentration.

The transient thermal phase grating technique has been successfully used to determine the energetics of very fast processes [11,16,17]. In this case, the time dependence of the refractive index change related to the thermo-induced variation of density is measured. Volume changes are also responsible for a variation of density. In organic liquids, their contribution to the density changes are substantially smaller than that of temperature [18], thus they will be neglected in the rest of this paper. As the grating fringes can be very small, this technique is the photothermal method offering the highest time resolution [19]. Recently, we have determined the free ion yields in bimolecular photoinduced electron transfer (ET) reactions using this technique [20]. The free ion yields were deduced from the heat released upon homogenous recombination of the free ions to the neutral ground state. The change of the shape of the thermal phase grating due to the second order kinetics of the heat release was assumed to have no influence on the maximum amplitude of the transient grating signal. This assumption was supported by the similarity of the free ion yields determined with the transient grating and those obtained from another method. The influence of the phase grating anharmonicity was taken into account in an investigation of iodine recombination by Zhu and Harris [21,22]. However, this more precise description of the grating shape renders the determination of the enthalpy of reaction from the signal very demanding.

In this paper, we investigate whether our previous assumption is reasonable, i.e. whether the grating anharmonicity can be neglected as long as only the signal amplitude is considered. We will show that this is the case, when an adequate experimental geometry is used.

2. Results and discussion

2.1. Population grating

In a photoinduced intermolecular ET reaction in a polar solvent such as acetonitrile, free ions are formed within a few nanoseconds upon dissociation of the geminate ion pair [23]. This process can be considered as instantaneous relative to the lifetime of the free ions and the time dependence of the free ion concentration [FI] can be described by a simple second order kinetics:

$$\frac{\mathrm{d}[\mathrm{FI}]}{\mathrm{d}t} = -2k_{\mathrm{rec}}[\mathrm{FI}]^2 \tag{3}$$

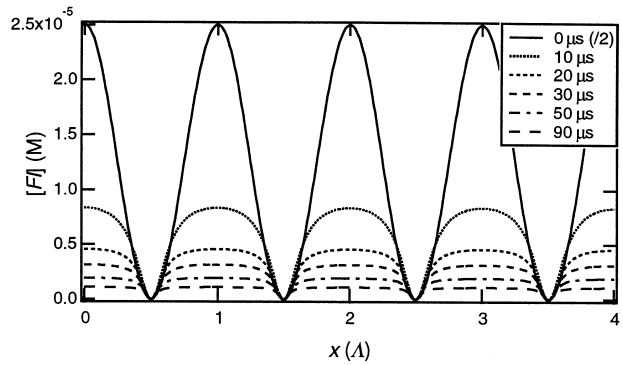

Fig. 1. Time dependence of the shape of the free ion population grating calculated using Eqs. (4) and (5).

where k_{rec} is the second order rate constant of homogeneous recombination. Considering that only encounters producing singlet geminate ion pairs can lead to a recombination to the neutral ground state, this constant is about four times smaller than the diffusion rate constant, i.e. about 5×10^9 $\mathrm{M}^{-1}\,\mathrm{s}^{-1}$ in MeCN at room temperature [24]. In a transient grating experiment, the excitation is spatially modulated and the concentration of the free ions varies along the modulation axis x. Therefore, the kinetics of [FI] depends on x:

$$[\mathrm{FI}](x,t) = \frac{[\mathrm{FI}]_0(x)}{1+2k_{\mathrm{rec}}[\mathrm{FI}]_0(x)t} \tag{4}$$

where $[\mathrm{FI}]_0(x)$ is the concentration of free ions directly after their formation, at a time defined here as $t=0$:

$$[\mathrm{FI}]_0(x) = \Delta[\mathrm{FI}]_0\cos\left(\frac{2\pi}{\Lambda}x\right) \tag{5}$$

where $\Delta[\mathrm{FI}]_0$ is the modulation amplitude of the free ion concentration at time zero. Fig. 1 illustrates the spatial distribution of the free ion population at different time delays after their formation, calculated from Eqs. (4) and (5). For this calculation, k_{rec} was taken as 5×10^9 $\mathrm{M}^{-1}\,\mathrm{s}^{-1}$ and $\Delta[\mathrm{FI}]_0$ as 5×10^{-5} M, a concentration corresponding to the experimental conditions used for the determination of the free ion yield [20]. As recombination is faster at the grating maxima, these peaks flatten with time and the concentration grating becomes strongly anharmonic. Such a grating can be described as a Fourier cosine series:

$$[\mathrm{FI}](x,t) = \frac{a_0(t)}{2} + \sum_{n=1}^{\infty} a_n(t)\cos\left(\frac{n2\pi}{\Lambda}x\right) \tag{6}$$

where the Fourier coefficients are given by

$$a_n(t) = \frac{1}{\Lambda}\int_{-\Lambda/2}^{\Lambda/2}[\mathrm{FI}](x,t)\,\cos\left(\frac{n2\pi}{\Lambda}x\right)\mathrm{d}x \quad n=0,1,2,3,\ldots \tag{7}$$

where $a_0(t)/2$ corresponds to the average concentration of free ions. The analytical solutions of this equation for a_0 and a_1 are

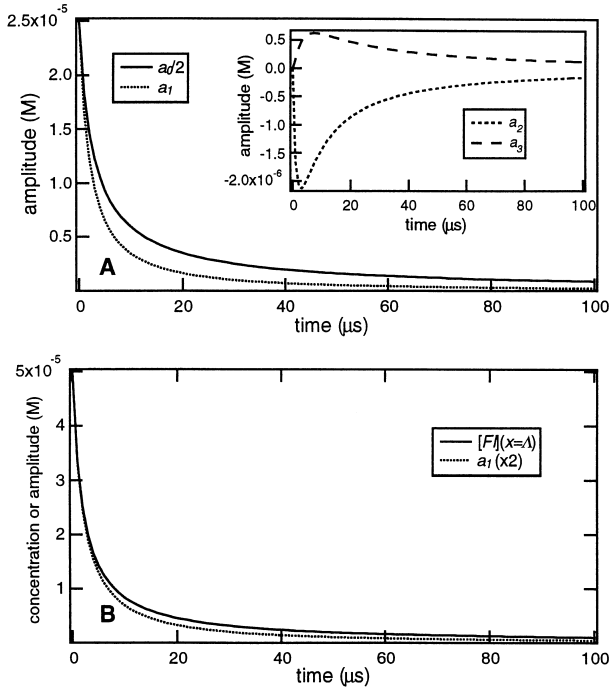

Fig. 2. (A) Time dependence of the four lowest a_n coefficients obtained from Fourier analysis of the free ion population grating. (B) Comparison of the time profile of the first order modulation amplitude of the free ion population grating a_1, with the decay of the free ion concentration at a grating peak [FI] ($x=\Lambda$).

$$a_0(t)=\frac{\kappa-1}{\kappa k_{rec}t} \tag{8}$$

$$a_1(t)=\frac{1-\kappa+\Delta[FI]_0 k_{rec}t}{\Delta[FI]_0\kappa(k_{rec}t)^2} \tag{9}$$

with

$$\kappa=(1+2\Delta[FI]_0 k_{rec}t)^{1/2} \tag{10}$$

Fig. 2 shows the time dependence of the four lowest Fourier coefficients obtained using Eqs. (8)–(10) or by numerical integration of Eq. (7). It can be seen that a_1 decreases substantially faster than $a_0/2$. The square of this coefficient is proportional to the diffracted intensity measured by probing at Bragg angle for first order diffraction. In the same way, the squares of higher order coefficients are proportional to the diffracted intensity measured at n times the Bragg angle for first order diffraction. It is immediately clear that the time dependence of a_1 does not reflect the decay of the average concentration of the free ions, $a_0/2$. The decay of a_1 is faster than that of $a_0/2$, because the first order grating contributes mostly to the grating peaks where the reaction is the fastest. Indeed, Fig. 2(B) shows the time profile of a_1 together with that of [FI] at a grating peak. The decay of a_1 is still faster, because it is not only due to the population decay but also to the transformation of the initially harmonic grating into an anharmonic grating. Consequently, the dynamics of a second order process *cannot* be extracted from the grating dynamics without taking its anharmonicity into account.

Experimentally, it is very difficult to detect these population gratings via the modulation of the absorbance or refractive index changes. Indeed, in the microsecond time scale, the thermal phase grating is formed and its contribution to the total diffraction efficiency is in most cases much larger than that of the amplitude and phase population gratings. If the transient population is very long lived, a possible solution to circumvent this problem is to take advantage of the fact that the decay of the thermal phase grating by thermal diffusion is faster than the decay of the population grating by translational diffusion [25]. Nevertheless, the free ions recombine in the microsecond timescale and thus the decay of the thermal phase grating has to be more than ten times faster to avoid any interference with the population grating. Such a fast decay would only be possible with unrealistically small fringes.

2.2. Thermal phase grating

Heat releasing processes result in a spatial modulation of the material strain $S(x)$ due to thermal expansion. If the heat release is instantaneous, counter-propagating acoustic waves are impulsively generated [26]. In this case, the time dependence of S can be considered as the response function of the system $R(t)$ [16,17]:

$$S(x,t)=S_0\cos\left(\frac{2\pi x}{\Lambda}\right)[1-\cos\omega t\exp(-\alpha v_s t)]$$

$$=S_0\cos\left(\frac{2\pi x}{\Lambda}\right)R(t) \tag{11}$$

where S_0 is the strain amplitude, v_s is the speed of sound, ω is the acoustic frequency ($\omega=2\pi v_s/\Lambda$) and α is the acoustic attenuation constant of the medium. The thermal phase grating experiment does not measure the strain but probes the changes of the refractive index. The latter is connected to strain through the optoelastic constant of the medium:

$$\Delta n=\rho(\partial n/\partial\rho)S \tag{12}$$

where ρ is the density of the solution. In the case of an instantaneous heat release, the time profile of the diffracted intensity exhibits an oscillation at a frequency ω caused by the propagation of the acoustic waves.

If the kinetics of the heat releasing process is not instantaneous, the time dependence of the refractive index change is proportional to the convolution of the response function with the rate of heat release $\dot{Q}$:

$$\Delta n(x,t)=C(x)\int_{-\infty}^{t}R(t-t')\dot{Q}(x,t')\,dt' \tag{13}$$

with

$$C(x)=\rho(\partial n/\partial\rho)S_0\cos\left(\frac{2\pi x}{\Lambda}\right) \tag{14}$$

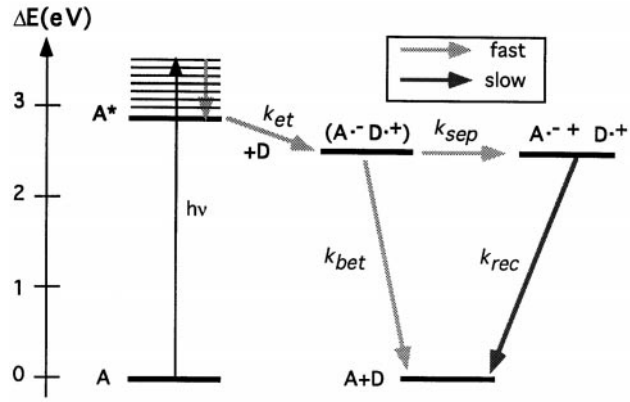

Fig. 3. Heat releasing processes involved in a photoinduced ET reaction between an excited electron acceptor A*, and an electron donor D, in a polar solvent. k_{et} is the pseudo-first order rate constant of ET quenching, k_{sep} is the rate constant of separation of the geminate ion pair to free ions and k_{bet} is the rate constant of back ET to the neutral ground state.

When the rate of heat release is slow compared with ω, the observed time profile of the diffracted intensity is free from oscillation, but in this case thermal diffusion has to be taken into account:

$$\Delta n(x,t) = C(x) \int_{-\infty}^{t} \exp(-k_{th}(t-t'))\dot{Q}(x,t')\,dt' \qquad (15)$$

where $k_{th} = D_{th}(2\pi/\Lambda)^2$ is the rate constant of thermal diffusion, D_{th} being the thermal diffusivity of the medium. If the crossing angle of the pump pulses is small enough, the fringe spacing can be large enough to slow down thermal diffusion well below the heat release. In this case, Eq. (15) can be approximated to

$$\Delta n(x,t) \approx C(x)Q(x,t)\exp(-k_{th}t) \qquad (16)$$

By choosing a proper fringe spacing, i.e. a suitable ω, the heat releasing processes can be separated into a fast (generating oscillation) and a slow process (oscillation free). If the energetics of one of these two processes is known, the energetics of the other can be determined by comparing the amplitude of the first oscillation maximum (fast heat) to the maximum amplitude of the time profile (fast + slow heat) [20]. This procedure does not require any fitting. For the determination of the free ion yields reported earlier, the acoustic frequency was chosen so as to separate the heat due to vibrational relaxation and free ion formation (fast heat) from that due to their homogeneous recombination (slow heat) [20] (see Fig. 3). All the processes involved in the fast heat release are first or pseudo-first order reactions and the corresponding thermal phase grating is harmonic. On the other hand, the time evolution of the slow heat Q_s is given by

$$Q_s(x,t) = \tfrac{1}{2}\{[\mathrm{FI}]_0(x) - [\mathrm{FI}](x,t)\}\Delta H_{rec} \qquad (17)$$

where ΔH_{rec} is the enthalpy of homogenous free ion recombination.

Fig. 4 shows the spatial distribution of Δn_s, the change of refractive index related to Q_s, at different time delays. Contrary to the population grating (see Fig. 1), the thermal phase grating is anharmonic as soon as it is formed. However, the degree of anharmonicity decreases as more ions recombine. Once the recombination is complete, the thermal phase grating is perfectly harmonic, reflecting the population grating at time zero. Using Eqs. (4), (16) and (17), $\Delta n_s(x,t)$ can also be expressed as a Fourier cosine series with coefficients b_n obtained by substituting $\Delta n_s(x,t)$ for $[\mathrm{FI}](x,t)$ in Eq. (7). In this case, b_0 and b_1 are given by

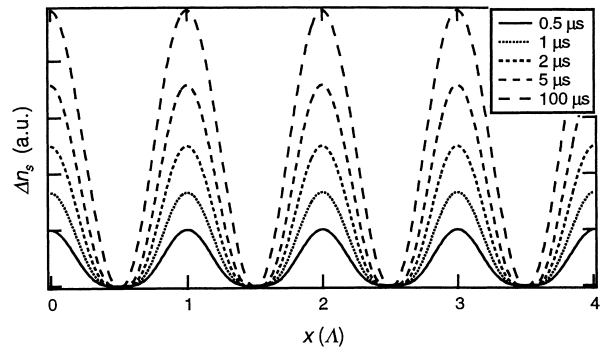

Fig. 4. Time dependence of the shape of the thermal phase grating due to free ion recombination calculated using Eqs. (16) and (17), without taking thermal diffusion into account.

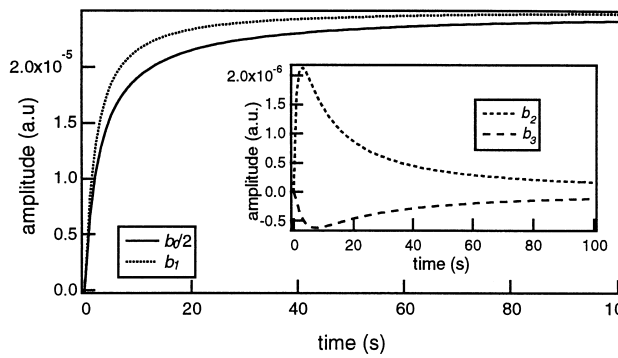

Fig. 5. Time dependence of the four lowest b_n coefficients obtained from Fourier analysis of the thermal phase grating without taking thermal diffusion into account.

$$b_0(t) = \frac{\Delta H_{rec}}{2}\left(\frac{1-\kappa(1-\Delta[\mathrm{FI}]_0)}{\kappa k_{rec}t}\right) \qquad (18)$$

$$b_1(t) = \frac{\Delta H_{rec}}{2}\left(\frac{\kappa(1+(\Delta[\mathrm{FI}]_0 k_{rec}t)^2) - \Delta[\mathrm{FI}]_0 k_{rec}t - 1}{\Delta[\mathrm{FI}]_0\kappa(k_{rec}t)^2}\right) \qquad (19)$$

The time dependence of the four lowest Fourier coefficients obtained using Eqs. (18) and (19) or by numerical integration are shown in Fig. 5. The higher order coefficients are similar to the a_n coefficients (Fig. 2), but have an opposite sign. The first order coefficient b_1 rises substantially faster than the average heat $b_0/2$. This can be explained in the same way as the difference between $a_0/2$ and a_1. However, the maximum amplitude of b_1 is the same as that of the average heat, although it is reached earlier in the first case. This indicates that, although the dynamics of the intensity diffracted

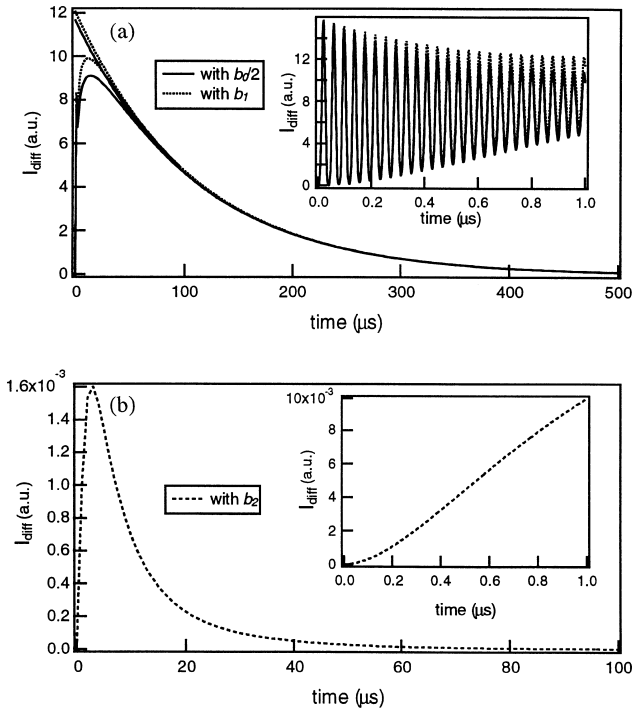

Fig. 6. (A) Time profiles of the diffracted intensity for a photoinduced ET process with a free ion yield of 0.5 and with $\Delta H_{rec} = 3.0$ eV, calculated with the coefficient b_1 for the slow heat release (anharmonic grating) and, for comparison, with $b_0/2$ (harmonic grating). The exponential functions extrapolated to time zero are used for determination of the total amount of heat released. Inset: diffracted intensity during the first microsecond. (B) Time profile of the intensity diffracted in the second order. Inset: detail of the first microsecond.

by the first order grating does not reflect that of the heat release, the maximum amplitude of the diffracted intensity is not influenced by the anharmonicity of the thermal grating.

Fig. 6(A) shows the time profile of the intensity diffracted in the first order simulated for the formation and decay of free ions in acetonitrile using Eqs. (16) and (2) with $A_1 = A_0 = 0$ and by replacing n_1 by the coefficient b_1 to describe the amplitude of the thermal grating caused by the slow heat release (see Fig. 3). For comparison, the diffracted intensity has also been calculated by assuming an harmonic thermal grating, i.e. by using $b_0/2$ for the slow heat release (dotted). For this simulation, the free ion yield, $\Phi_{ion} = Q_s/\Delta H_{rec}$, is taken as 0.5, the enthalpy of recombination is $\Delta H_{rec} = 3.0$ eV and the total amount of heat released is 3.5 eV, corresponding to the energy of a 355 nm photon. The transient grating parameters are the same as those used to determine the free ion yields, i.e. $\Lambda = 3.8 \times 10^{-5}$ m and $\omega = 1.8 \times 10^8\ s^{-1}$, corresponding to excitation at 355 nm with a crossing angle θ of about 0.54° [20]. The inset of Fig. 6(A) shows the first microsecond where the damping of the oscillation due to the fast heat release down to a quarter of the initial peak intensity takes place via acoustic attenuation. With the crossing angle used, the thermal diffusion which is responsible for the decay of the diffracted intensity is slow ($k_{th} = 4.7 \times 10^3\ s^{-1}$), but an increase of the angle up to $\theta = 4.8°$ results in a 100 fold increase of k_{th}. By comparing the amplitude of the first oscillation maximum to the maximum amplitude of the time profile extrapolated to time zero as described in detail in ref. [20], the ion yield obtained from the diffracted intensity simulated with the anharmonic grating amounts to 0.49, while it is equal to 0.47 if the average slow heat is used. This smaller value is due to the fact that the maximum amplitude with $b_0/2$ is reached when the decay of the thermal grating has progressed further than with b_1. This effect illustrates the main problem arising with second order heat releasing processes, i.e. the very long time required for the process to be completed. To obtain an extrapolated value corresponding to the total amount of heat released, the thermal diffusion has to be as slow as possible. For example, a ten fold increase of k_{th}, obtained by opening the crossing angle from 0.54° to 1.63°, results in an apparent free ion yield of 0.44. In this case k_{th} becomes large, and Eq. (16) is no longer valid. The correct ion yield can only be determined by fitting Eq. (2) with Eq. (15) to the time profile.

The slow heat release can of course be accelerated by increasing the initial concentration of free ions. However the high excitation intensity required can lead to the saturation of the grating and to the occurrence of biphotonic processes. In this case, the population grating is already anharmonic at time zero [27]. Moreover, biphotonic processes have absolutely to be avoided in order to extract the correct energetic parameters from the measured signal.

Finally, Fig. 6(B) shows the simulated time profile of the intensity measured by probing the grating at twice the Bragg angle for first order diffraction. This signal does not exhibit the initial oscillatory behaviour, for only the thermal phase grating due to the slow heat release has a non-zero b_2 coefficient. Compared with the signal diffracted in the first order, its amplitude is about 1000 times smaller. This signal is so weak that it could not be observed experimentally with the set-up described in ref. [20]. A diffracted signal was measured in the second order only with a high excitation intensity (about 6 mJ cm^{-2}). However, the time profile exhibited the initial oscillation, indicating that the population grating was already anharmonic at time zero owing to saturation.

3. Concluding remarks

In this paper, we have investigated the limits of the transient grating technique for investigating processes following second order kinetics. Owing to the time dependence of the grating shape, the dynamics of the process *cannot* be deduced directly from the time profile of the diffracted intensity. However, the departure of the measured dynamics from that of the concentration at the grating peaks is small as shown in Fig. 2(B). The energetics of second order processes such as free ion recombination *can* be deduced accurately from the maximum amplitude of the diffracted intensity without taking the anharmonicity of the grating into account, as long as thermal diffusion is slow. This is achieved by using crossing angles below 1° for an excitation wavelength of 355 nm.

Larger angles would lead to an underestimation of the free ion yield.

If the free ion yield is known but the enthalpy of the recombination is investigated, too large an angle would also lead to an underestimation of ΔH_{rec}.

The study presented here supports the results obtained in previous investigations of free ion recombination [20,28], as the experimental conditions described above were met. Should these conditions not be satisfied, the energetics of the recombination would only be obtained by fitting Eq. (2) with Eq. (15) to the measured time profile.

Acknowledgements

This work was supported by the 'Fonds national suisse de la recherche scientifique' through project number 20-41855.94 and by the 'programme d'encouragement à la relève universitaire de la Confédération'. Financial support form the 'Fonds de la recherche' and the 'Conseil de l'Université de Fribourg' is also acknowledged.

References

[1] H.J. Eichler, P. Günter, D.W. Pohl, Laser-Induced Dynamic Gratings, Springer Verlag, Berlin, 1986.
[2] J.R. Salcedo, A.E. Siegman, D.D. Dlott, M.D. Fayer, Phys. Rev. Lett. 41 (1978).
[3] L. Gomez-Jahn, J. Kasinski, R.J.D. Miller, Chem. Phys. Lett. 125 (1986).
[4] M. Terazima, K. Okamoto, N. Hirota, J. Chem. Phys. 102 (1995) 2506.
[5] G.A. Kenney-Wallace, S. Wallace, IEEE J. Quantum Electron. 19 (1983) 719.
[6] F.W. Deeg, J.J. Stankus, S.R. Greenfield, V.J. Newell, M.D. Fayer, J. Chem. Phys. 90 (1989) 6893.
[7] D.W. Phillion, D.J. Kuizenga, A.E. Siegman, Appl. Phys. Lett. 27 (1975) 85.
[8] E. Vauthey, Chem. Phys. 196 (1995) 569.
[9] R.S. Moog, M.D. Ediger, S.G. Boxer, M.D. Fayer, J. Phys. Chem. 86 (1982) 4694.
[10] J.-L. Gumy, E. Vauthey, J. Phys. Chem. 100 (1996) 8628.
[11] E. Vauthey, A. Henseler, J. Phys. Chem. 99 (1995) 8652.
[12] E. Vauthey, J. Phys. Chem. A, 101 (1997) 1635.
[13] D.M. Burland, C. Bräuchle, J. Chem. Phys. 78 (1982) 4502.
[14] H. Kogelnik, Bell System Tech. J. 48 (1969) 2909.
[15] M. Samoc, P.N. Prasad, J. Chem. Phys. 91 (1989) 6643.
[16] L. Genberg, Q. Bao, S. Gracewski, R.J.D. Miller, Chem. Phys. 131 (1989) 81.
[17] M.B. Zimmt, Chem. Phys. Lett. 160 (1989) 564.
[18] J. Morais, J. Ma, M.B. Zimmt, J. Phys. Chem. 95 (1991) 3887.
[19] S.E. Braslavsky, G.E. Heibel, Chem. Rev. 92 (1992) 1381.
[20] A. Henseler, E. Vauthey, J. Photochem. Photobiol. A: Chem. 91 (1995) 7.
[21] X.R. Zhu, J.M. Harris, Chem. Phys. 157 (1991) 409.
[22] X.R. Zhu, J.M. Harris, Chem. Phys. Lett. 186 (1991) 183.
[23] N. Mataga, T. Asahi, Y. Kanda, T. Okada, T. Kakitani, Chem. Phys. 127 (1988) 249.
[24] E. Haselbach, E. Vauthey, P. Suppan, Tetrahedron 44 (1988) 7335.
[25] T. Hara, N. Hirota, M. Terazima, J. Phys. Chem. 100 (1996) 10194.
[26] K.A. Nelson, R. Casalegno, R.J.D. Miller, M.D. Fayer, J. Chem. Phys. 77 (1982) 1144.
[27] X.R. Zhu, J.M. Harris, J. Phys. Chem. 93 (1989) 75.
[28] E. Vauthey, A. Henseler, J. Photochem. Photobiol. A: Chem., in press.